Hydrodynamic Interactions between swimming microorganisms in a linearly density stratified fluid

Rishabh V. More and Arezoo M. Ardekani*

School of Mechanical Engineering, Purdue University, West Lafayette, IN 47907, USA.

(Dated: March 2, 2021)

Abstract

Oceans and lakes sustain intense biological activity due to the motion of marine organisms which has significant ecological and environmental impacts. The motion of individual organisms and their interactions with each other play a significant role in the collective motion of swimming organisms. However, ubiquitous vertical density stratification in these aquatic environments significantly alters the swimmer interactions as compared to in a homogeneous fluid. Furthermore, organisms have sizes varying over a wide range which results in finite inertia. To this end, we numerically investigate the interactions between a pair of model swimming organisms in two configurations: 1) approaching each other, & 2) moving side-by-side with finite inertia in a linearly density stratified fluid. We use the archetypal reduced-order squirmer model to numerically model the swimming organisms. We present trajectories and the contact times of interacting squirmer (puller & pusher) pairs for different Re in the range 1-50 and Ri in the range 0-10. Depending on the squirmer Re and Ri we observe that the squirmer interactions can be categorized as i) pullers getting trapped in circular loops at high Re and low Ri, ii) pullers escaping each other with separating angle decreasing with increasing stratification at low Re and high Ri, iii) pushers sticking to each other after the collision and deflecting away from the collision plane for either low Re or high Ri, iv) pushers escaping otherwise with an angle of separation increasing with stratification. Stratification also increases the contact time for squirmer pairs. The results presented can be useful in understanding the mechanisms behind the accumulation of planktonic organisms in horizontal layers in a stratified environment like oceans and lakes.

I. INTRODUCTION

The sizes of swimming organisms span a wide range of length scales from micrometers to a few meters. Thus, depending on their size these organisms employ a variety of swimming mechanisms that take advantage of the fluid flow around them to propel themselves. In a fluid with a characteristic density ρ_0 and dynamic viscosity μ, the Reynolds number for an organism of size a and moving with a speed U_0, is defined as $\mathrm{Re} = \rho_0 U_0 a/\mu$, which is the ratio of inertial to viscous forces. At micro scales, $\mathrm{Re} \approx 0$ and the microorganisms make use

* ardekani@purdue.edu.

of the viscous drag exerted by the fluid to move. Larger organisms like fishes and whales have a finite Re and utilize the lift generated by the accelerating fluid past them to swim.

In the recent years, researchers have devoted significant effort to investigate the collective dynamics of organisms. Dense suspensions of bacteria on scales much larger than a cell in the Stokes flow limit exhibit transient, reconstituting, high-speed jets straddled by vortex streets [1], self sustained turbulence [2], extended spatio-temporal coherent dynamics [3], and superdiffusion in short times [4]. The collective motion of the bacteria is determined by short-range pair interactions at high concentrations [2]. Even at high Re, e.g., schooling fish, flocking birds and swarming insects, the hydrodynamic interaction between the moving organisms and their detached vortical structures significantly affect the swimming (flying) efficiency [5, 6].

Many studies on the collective behavior of swimmers neglect the near-field hydrodynamic interactions and only consider the far-field interactions to simulate the dynamics of swimmer suspensions [7, 8]. But, to completely understand the collective behavior of the micro-swimmers, it is important to investigate the near-field hydrodynamics between a pair of interacting swimmers. It is well known that, in the dilute limit, micro-swimmers behave as a force dipole leading to a velocity field decaying as $1/r^2$, where r is the distance from the micro-swimmer [9]. Due to the slow decay of the induced velocity field, the pairwise interaction between two swimmers cannot be neglected even at large separations. Various experimental studies have shown the crucial role of hydrodynamic interactions between microorganisms in determining their dynamics, e.g., dancing *Volvox* [10], interacting pair of *Paramecia* [11], the formation of dynamic clusters in suspensions of motile bacteria [12] and hydrodynamic self-mediation of bacteria into two-dimensional crystals [13].

Many theoretical and numerical studies have also been conducted to investigate the hydrodynamic interactions between two model swimmers. Pullers (pulled from the front) are attracted towards each other first which leads to near contact and changes in their swimming orientations to finally separate [14, 15]. Two self-propelling bacteria by rotating helical flagella avoid each other by changing their orientations [16]. The swimmer-swimmer interaction is complex and strongly affected by their relative displacement, orientation, initial configuration and swimming stroke phase. Slight variations in these parameters lead to different scattering angles, swimming speeds and a range of different interactions, such as attraction, repulsion, or oscillation [17–20]. Hydrodynamic interactions between two microswimmers

also lead to the the enhancement of the swimming efficiency by synchronizing the phase of two adjacent flagella [21]. However, all these studies however were performed in the Stokes regime assuming $\mathrm{Re} = 0$ without considering the effect of swimmer inertia.

For swimming microorganisms, the Re ranges from 10^{-4} for bacteria [22], 10^{-3} for *Chlamydomonas*, $0.01-0.1$ for *Volvox* [10], $0.1-1$ for freely swimming zooplankton *Daphnia magna* [23], $0.2-2$ for *Paramecia* depending on swimming or escaping mode [11], $O(10)$ for *Pleurobrachia*, and $20-150$ for copepods [24]. Thus, it is crucial to know the influence of finite inertia on the hydrodynamic interactions of two swimmers. Theoretical and computational studies on the locomotion of an individual swimmer with finite inertia [25, 26] further indicate that inertia can lead to notable differences in the swimming dynamics of swimmers. Inertia also affects the hydrodynamic interactions between swimmer pairs. Puller and pusher pairs either separate away from each other or get trapped near each other depending on their Re and swimming modes [27].

Many swimming organisms with low to intermediate Re are abundant in oceans and lakes and their motion results in intense biological activity in these aquatic bodies. Hence studying the interactions of organisms is an intriguing problem having wide implications for ocean ecology [28]. However, understanding the physics behind these phenomenon is a complex undertaking as vertical variations in water density are ubiquitous in aquatic and marine environments [29], due to gradients in temperature (thermoclines) or salinity (haloclines). These density variations with depth can manifest themselves in a gamut of environmental and oceanographic processes [30–33]. Even though the stratification length scale is $O(m)$, the appropriate length scale to determine whether stratification affects the motion of the swimmers is $O(100)$ μm [34]. Marine microplankton with sizes ranging from $20-200$ μm are abundant in such a stratified environments along with other meso-, macro- and mega-planktonic organisms which have Re ranging from $O(0.01-100)$ [35]. These observations insinuate the significant role of stratification in governing the locomotion of individual organisms as well as the interaction between two close organisms in the mentioned size range.

Much like inertia, stratification also significantly affects the motion of micro-swimmers. At low Re, the vertical migration of small organisms is hydrodynamically affected due to the rapid velocity decay as well as a higher energy expenditure in stratified fluids [36, 37]. At a finite Re, stratification even leads to striking differences in the swimming speeds and stability

of swimmers as compared to their motion in a homogeneous fluid [38]. The collective vertical migration of swimmers in a stratified fluid generates aggregation-scale eddies which can potentially alter the physical and bio-geo-chemical structure of the water column [32, 39, 40]. Stratification also leads to the accumulation of marine organisms like plankton [41, 42]. Thus, investigating the combined effect of inertia and stratification on the interaction between a pair of interacting swimmers is a non-trivial and interesting problem that we address in this paper.

Looking at the interactions between a pair of organisms is crucial for modeling the collective dynamics of marine organisms, e.g., migrating swimmer schools in stratified environments. To this end, we numerically investigate the effect of density stratification on the interactions between a pair of inertial swimmers. We model the swimmers using the archetypal spherical squirmer model which is explained in detail in Sec. II B. But first, we present the governing equations and the computational methodology used to solve these equations in Sec. II A. Then we discuss the findings of the simulations in Sec. III.

II. GOVERNING EQUATIONS AND COMPUTATIONAL METHODOLOGY

We consider a pair of interacting squirmers moving through an incompressible Newtonian viscous fluid. The governing equations and the numerical procedure implemented to simulate the motion a pair of interacting squirmers through a linearly stratified fluid at finite Re are presented in this section. We consider a linearly density stratified fluid such that the density increases in the downward z direction and the gravity is acting in the downward z direction as shown in fig. 1. The following subsections explain the governing equations and the numerical schemes used to solve them in details.

A. Flow and density fields:

The fluid flow is governed by the Navier-Stokes equations for an incompressible Newtonian fluid and these equations are solved in the entire domain, Ω. We simplify the Navier-Stokes equations for a fluid flow of a density stratified fluid using the Boussinesq approximation. The resulting equations can be written as,

$$\rho_0 \frac{\mathrm{D}\mathbf{u}}{\mathrm{D}t} = -\nabla P + \mu \nabla^2 \mathbf{u} + (\rho - \bar{\rho})\mathbf{g} + \mathbf{f}, \text{ in } \mathbf{\Omega}, \tag{1}$$

$$\nabla \cdot \mathbf{u} = \mathbf{0}, \text{ in } \mathbf{\Omega}, \tag{2}$$

where t is the time, $\mathbf{u}$ is the velocity vector, P is the hydrodynamic pressure, $\mathbf{g}$ is the acceleration due to gravity, μ is the dynamic viscosity of the fluid, ρ_0 is the reference fluid density and $\bar{\rho}$ is the volumetric average of the density over the entire domain. $D(\cdot)/Dt$ is the material derivative. ρ is the local density at the grid point. We use the phase indicator function ψ which is 1 inside the squirmer and 0 outside to mark the squirmer domain. The subscript f stands for fluid and s for squirmer. $\mathbf{f}$ in equation 1 is the body force which accounts for fluid-solid interactions in the Distributed Lagrange Multiplier (DLM) method [43]. DLM has been widely used in the literature to simulate the motion of rigid particles and model swimmers in both homogeneous and stratified fluids [27, 32, 44–46].

The density field evolution is governed by the following advection-diffusion equation,

$$\frac{\mathrm{D}\rho}{\mathrm{D}t} = \kappa \nabla^2 \rho, \text{ in } \Omega, \tag{3}$$

here κ is the diffusivity of the stratifying agent and ρ is the density field. We define Prandtl number $\mathrm{Pr} = \nu/\kappa$, which is the ratio of the momentum diffusivity to the diffusivity of the stratifying agent. We split the density into two parts: i) the initial linear background density profile, $\bar{\rho}(z)$, and ii) the density perturbation induced by the motion of the squirmers, $\rho^{'}$. So,

$$\rho = \bar{\rho}(z) + \rho^{'}. \tag{4}$$

Here, the initial density of the fluid varies linearly with depth z as $\bar{\rho}(z) = \rho_0 - \gamma(z - z_0)$, where γ is the vertical density gradient and z_0 is the location with reference density ρ_0. The stratification strength can be quantified by the Brunt–Väisälä frequency, $N = (\gamma g/\rho_0)^{1/2}$, the natural frequency of oscillation of a vertically displaced fluid parcel in a stratified fluid. Substituting eq. 4 in eq. 3 we obtain the following temporal and spatial evolution equation for the density perturbation, $\rho^{'}$,

$$\frac{\mathrm{D}\rho^{'}}{\mathrm{D}t} = -\mathbf{u} \cdot \nabla \bar{\rho}(z) + \kappa \nabla^2 \rho^{'}, \text{ in } \Omega. \tag{5}$$

We solve the advection-diffusion equation for the density perturbation, $\rho^{'}$ and add it to the initial linear density profile to calculate the density field as shown in eq. 4.

We use a finite volume method [47] to discretize the equations 1-2 and 5 on a non-uniform staggered Cartesian fixed grid. We use a second order quasi Crank-Nicolson method

for temporal evolution. Convection and diffusion terms in the momentum equation have been solved using a QUICK (quadratic upstream interpolation for convective kinetics) and central-difference schemes [48], respectively. Both convection and diffusion terms in the density perturbation, $\rho^{'}$, equation have been discretized using the central difference scheme [32]. The numerical tool utilized for this study is based on the earlier version of PARIS [47]. We use periodic boundary conditions for velocity components and the density perturbation in all the three directions.

B. Swimmer model:

Mathematically modelling the motion of a real micro-organism is an enormously convoluted undertaking. This is due to the existence of a wide variety of length scales (roughly $O(1)$ – $O(1000)\mu m$ for common marine species), multitudes of swimming, grazing and other behaviors depending on a range of parameters relating to their environments. In addition, these organisms exhibit a vast variety of shapes which might even not be the same as individual micro-organisms change their shapes to feed, reproduce or protect themselves from predators or hostile environments. Thus, we need to make several simplifications, even for the simplest micro-organisms in order to mathematically model and analyse them [22]. Hence, by necessity, we use a reduced order squirmer model which is primitive. This model, however simple it may be, still includes important aspects of micro-organism hydrodynamics such as, it swims and has a finite size so that excluded-volume effects and hydrodynamic interactions can be analysed non-trivially.

The squirmer model [49, 50] has been widely used as a model for swimmers like *Volvox* in the literature [51]. In the earlier studies, researchers utilized the squirmer model to investigate the motion of self-propelled organisms in a viscosity dominated flow regime, i.e., $\mathrm{Re} \to 0$. This allowed researchers to investigate various problems in a non-inertial regime, such as, the nutrient uptake by self-propelled organisms [52], the hydrodynamic interactions between two squirmers [11], rheology of suspensions of squirmers [53], mixing by swimmers [54] as well as swimming in non-Newtonian fluids [55, 56] using the squirmer model. Recently, researchers have studied the effect of finite inertia on the motion of swimmers by extending the squirmer model to low and intermediate Re number regimes [25–27, 32, 57, 58]. The squirmer model was also used to study the effect of fluid density stratification on the

motion of an individual squirmer [36, 38] and the biogenic mixing induced by a swarm of swimming organisms [32] with low to intermediate Re. Thus, the squirmer model, owing to its simplicity and germane representation of the flow field generated by the self-propelling ciliary organisms, opens up a wide range of avenues for studying self-propulsion in various environmental conditions.

The squirmer self-propels by wavelike motion of its surface. The spherical squirmer model, first introduced by Lighthill [49] and later modified by Blake [50] mimics the self-propulsion produced by the coordinated beating of dense array of cilia on its surface. These axisymmetric ciliary deformations result in the radial (u_r^s) and the tangential (u_θ^s) surface velocity components in a frame of reference attached to the squirmer with radius a:

$$u_r^s|_{r=a} = \sum_{n=0}^{\infty} A_n(t) P_n(\cos\theta), \tag{6}$$

$$u_\theta^s|_{r=a} = \sum_{n=1}^{\infty} \frac{-2}{n(n+1)} B_n(t) P_n^1(\cos\theta), \tag{7}$$

respectively. Here, r is the distance from the center of the squirmer, θ is the angle measured from the direction of the locomotion, A_n and B_n are the time dependent amplitudes of ciliary deformations and P_n, P_n^1 are the associated Legendre polynomials of degree n. The swimming speed of a neutrally buoyant squirmer at $\mathrm{Re} = 0$, i.e., in a Stokes flow depends only on the first mode of each surface velocity component and is given by, $U_0 = (2B_1 - A_1)/3$. This swimming speed is independent of fluid viscosity and other swimming modes [49].

For this study we consider a reduced order squirmer which has no radial velocity and only the first two modes of the surface tangential velocity,

$$u_\theta^s(\theta) = B_1 \sin\theta + B_2 \sin\theta\cos\theta, \tag{8}$$

where θ is the angle with respect to the swimming direction, and B_1 and B_2 are the first two squirming modes. The ratio, $\beta = B_2/B_1$, determines whether the squirmer is neutral ($\beta = 0$) or a puller ($\beta > 0$) or a pusher ($\beta < 0$). In the Stokes flow limit, the velocity of a squirmer in an unbounded domain is $U_0 = 2B_1/3$, we use this as the velocity scale in this study. To impose the above given tangential velocity on the surface of the squirmer, we set

the following divergence free velocity field inside the squirmer [57],

$$\begin{aligned}\mathbf{u}_{in} = &\left[\left(\frac{r}{a}\right)^m - \left(\frac{r}{a}\right)^{m+1}\right]\left(u_\theta^s \cot\theta + \frac{du_\theta^s}{d\theta}\right)\mathbf{e}_r \\ &+ \left[(m+3)\left(\frac{r}{a}\right)^{m+1} - (m+2)\left(\frac{r}{a}\right)^m\right] u_\theta^s \mathbf{e}_\theta,\end{aligned} \tag{9}$$

here a is the radius of the squirmer, r is the distance from the squirmer's center, $\mathbf{e}_r$ and $\mathbf{e}_\theta$ are the unit vectors in the radial and polar directions, and m is an arbitrary integer. The simulation results do not depend on the choice of m. The squirmer velocity is calculated by solving the following equations:

$$\mathbf{U} = \frac{1}{M_s}\int_{V_s} \rho_s(\mathbf{u} - \mathbf{u}_{in})dV, \tag{10}$$

$$\mathbf{I_s} \cdot \boldsymbol{\omega} = \int_{V_s} \mathbf{r} \times \rho_s(\mathbf{u} - \mathbf{u}_{in})dV, \tag{11}$$

where V_s, M_s, and $\mathbf{I_s}$ are volume, mass and the moment of inertia of the squirmer. $\mathbf{U}$ and $\boldsymbol{\omega}$ are the translational and the rotational velocities of the squirmer. Finally, the force $\mathbf{f}$ is calculated by the following iterative formula:

$$\mathbf{f} = \mathbf{f}^* + \alpha\frac{\rho\psi}{\Delta t}(\mathbf{U} + \boldsymbol{\omega} \times \mathbf{r} + \mathbf{u}_{in} - \mathbf{u}), \tag{12}$$

where $\mathbf{f}^*$ is the force calculated in the previous iteration and α is a dimensionless factor chosen in such a way that iterations for calculating $\mathbf{f}$ converge quickly [27, 46]. Many organisms utilize techniques like gas vesicles [59], carbohydrate ballasting [60], and ion replacement [61, 62] for buoyancy control. Hence, for this study in order to isolate the effect of stratification on the motion of a squirmer, we consider the squirmer to be neutrally buoyant, i.e., the net buoyancy force acting on the squirmers due to differences in their density and the density of the fluid is zero at any instance of time. This is achieved by equating the density field inside the squirmer domain to the instantaneous background fluid density at that location ($\rho_s(\mathbf{x}, t) = \bar{\rho}(\mathbf{x}) + \rho^{'}(\mathbf{x}, t)$, where $\mathbf{x}$ is any location inside the squirmer domain). The same condition for neutral buoyancy was used for investigating the swimming dynamics of an individual squirmer with finite inertia in a stratified fluid [38]. In addition, we assume the κ to be uniform and the same for the squirmer and the background fluid [32, 63].

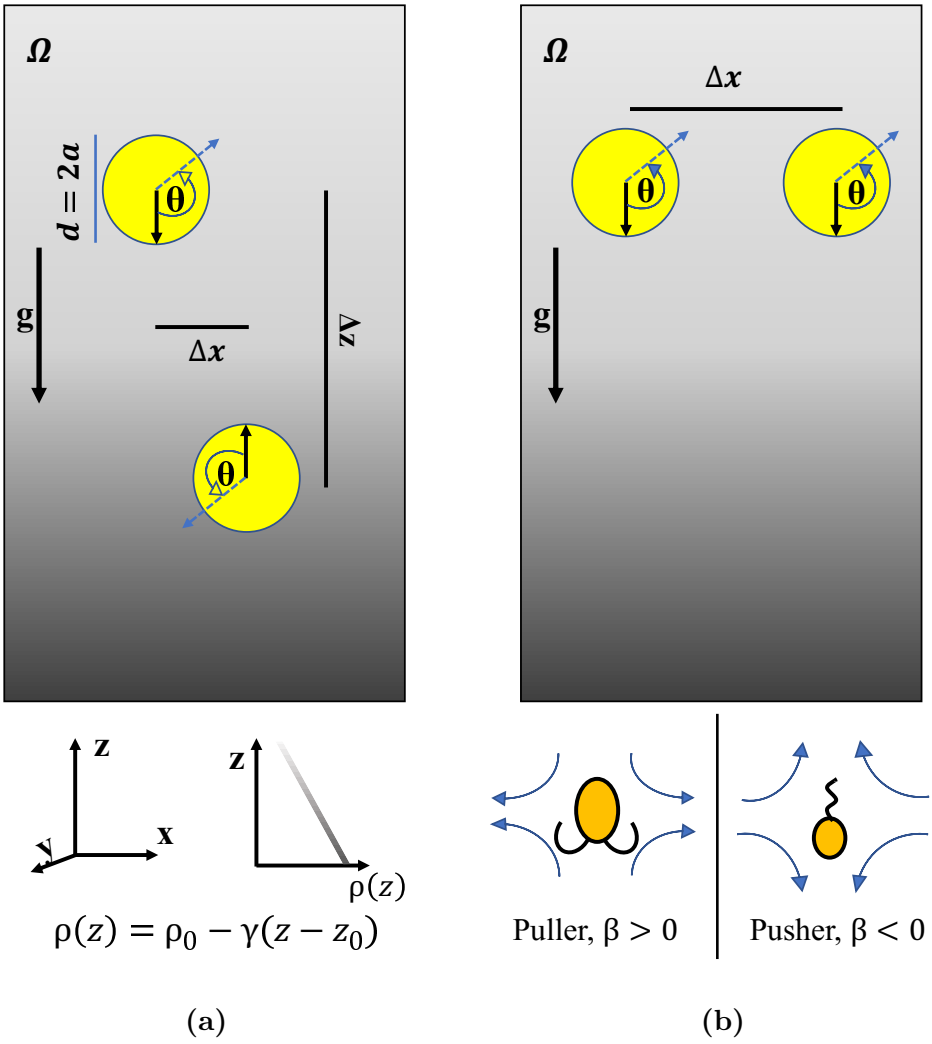

FIG. 1 Problem schematic: a) Initial conditions for the pair of squirmers approaching each other in a linearly stratified fluid. b) Initial conditions for a pair of squirmers moving side-by-side in a stratified fluid. The cartoons at the bottom in (b) show the flow fields generated by pullers ($\beta > 0$) and pushers ($\beta < 0$) as they move. The arrows in the squirmer bodies show their initial orientations. Darker shade of grey indicates higher density.

C. Simulation conditions

We explore the interactions of two squirmers moving towards each other leading to collision and two squirmers moving in the same direction side by side. We normalize the spatial parameters with the squirmer radius a, the velocities with U_0 and the time with the time

scale a/U_0. We denote the dimensionless time with T.

The first case considered is that of a pair of squirmers approaching each other in opposite directions so that they collide. In this case, the squirmers are initialized at a center to center distance Δz and Δx in the z and x directions, respectively in the plane $y = 0$. Their initial orientations are such that they are moving in opposite directions facing each other. We set $\Delta z = 8$ and $\Delta x = 1$, unless stated otherwise (see fig. 1a).

In the second case, where the squirmers are moving in the same direction side by side, we initialize them at the same initial vertical location z_i, separated by a center to center distance Δx in the x direction in the plane $y = 0$. We set $\Delta x = 4$, unless mentioned otherwise (see fig. 1b).

An earlier study in a homogeneous fluid considered only a colliding pair of squirmers in which the squirmers swim in opposite direction [27]. We, however, consider colliding as well as side-by-side configuration which covers squirmers moving opposite to each other as well as moving in the same direction. Also, the vertical direction is the preferred direction because in many real-life situations, the swimmers move in the vertical direction such that they are parallel to the direction of the stratification or gravity mainly for grazing or in the search of the sunlight during their diel cycles [64, 65]. In addition, the direction of the motion considered in this study is one of the common situations for swimmers moving in oceans, e.g. bioconvection [66]. So, we initialize the squirmers with their initial orientations parallel to the direction of gravity, i.e. downwards or upwards.

When the squirmers approach very close to each other, the high pressure in the thin film between the squirmers prevents any non-physical overlaps. However, a very small grid resolution is needed to resolve the thin liquid film and consequently it is computationally expensive. A repulsive force is imposed during the collision to prevent the non-physical overlap [27, 43],

$$\mathbf{F}_r = \frac{C_m}{\epsilon}\left(\frac{D-d-dr}{dr}\right)^2 \mathbf{n}, \tag{13}$$

where $\epsilon = 10^{-4}$ is a small positive number, D is the distance between two squirmers, $C_m = M_s U_0^2/a$ is the characteristic force, $d = 2a$ is the minimum possible distance, and dr is the force range and is set to be twice the smallest grid size Δ. The direction of the repulsive force $\mathbf{n}$ is along the squirmers' line of centers.

We carry out simulations for pushers and pullers with β = -5 and 5, respectively. The Re

for the squirmers were varied between $1 - 50$. To study the effects of stratification on the interaction of two inertial squirmers, we vary the Richardson number, $\mathrm{Ri} = \rho_0 a^3 N^2/\mu U_0$, which quantifies the relative importance of the buoyancy and the viscous forces, between $0 - 10$. The domain size for this study is $40a \times 20a \times 40a$ for colliding squirmers case while the domain size is $40a \times 20a \times 80a$ for the side-by-side case. The smallest grid size was chosen such that there are around 35 grid points in one squirmer diameter, i.e., $\Delta \approx d/35$. This grid size was found to be enough to resolve both the velocity and density boundary layers around the squirmers for the chosen Re range and $\mathrm{Pr} = 0.7$. We present the grid independence tests in appendix A.

It should be noted that we use $\mathrm{Pr} = 0.7$ for this study rather than $\mathrm{Pr} = 7$ or $\mathrm{Pr} = 700$ which are the Pr values for a temperature stratified water and a salt stratified water, respectively. This has been done mainly to save the computational costs incurred by setting high values of Pr. In a stratified fluid, a density boundary layer is present in addition to the velocity boundary layer near the squirmer's surface. The thickness of this density boundary layer scales as $\approx O(d/\sqrt{\mathrm{RePr}})$. For accurate resolution of the flow within this boundary layer, it is necessary to have at least a few grid points in it. This imposes limitations on the maximum mesh size that can be used for the simulations. Owing to large size of the domain, using such a fine grid becomes computationally expensive. Hence, we use a smaller value for the Pr which enables us to resolve the fluid flow as well as the density field in both the boundary layer and the outside. It has been shown in previous studies that, changing the value of Pr merely changes the magnitudes of the velocities of the objects [46] and squirmers [38] moving in a stratified fluid conserving the overall qualitative trends and behaviors. We discuss more on this in Sec. III E.

III. RESULTS AND DISCUSSION:

This section presents the important results from the simulations. We also present results on the interactions of pair of inertial squirmers in a homogeneous fluid. The comparison between the trajectories of the squirmers and their velocities in the two distinct fluids allows us to investigate the effect of density stratification on the squirmer pair interactions.

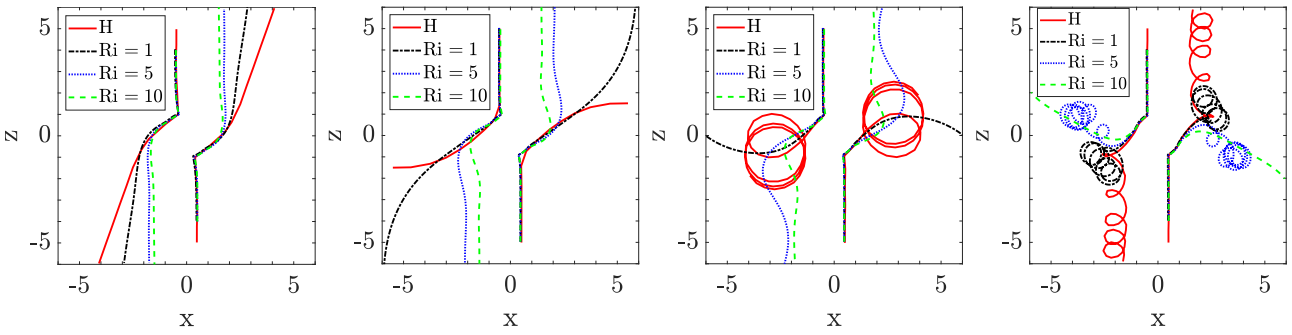

(a) Re = 1 **(b)** Re = 5 **(c)** Re = 10 **(d)** Re = 50

FIG. 2 Trajectories for colliding pullers with $\beta = 5$ in a homogeneous and a stratified fluid with increasing stratification strengths. At low Re (1 and 5), stratification leads to reorientation of the pullers after the collision. For higher Re values (10 and 50), stratification results in the elimination of the close loop trajectories observed in a homogeneous fluid after the collision of two pullers. *H* in the legends stands for homogeneous fluid or Ri = 0.

A. Pairwise interactions of pullers in a stratified fluid

1. *Pullers approaching each other*

Fig. 2 shows the trajectories for two pullers approaching each other in opposite directions, initially oriented parallel to each other for Re = 1, 5, 10 and 50 in a homogeneous fluid and a stratified fluid with Ri = 1, 5 and 10. In the absence of any density stratification, the trajectories of the colliding pullers reveal three patterns based on the magnitude of Re. At relatively low values of Re, i.e. 1 and 5, the pullers scatter away from each other with a positive scattering angle, ϕ, measured with respect to initial squirmer orientation. With increasing Re, i.e., from Re = 1 to Re = 5, ϕ increases from $\approx 20°$ to a value just less than 90°. As we increase the Re further to a higher value of 10, the pullers do not escape each other after the collision, but are trapped in clockwise loops with radii $\approx 2a$. At an even higher Re = 50, the pullers are no longer trapped but escape with $\phi \approx 0°$ but keep on rotating in clockwise loops with diminished radii compared to Re = 10 case.

Introducing stratification results in distinct changes in the trajectories of the interacting pullers depending on their Re and the stratification strength, i.e., Ri. Stratification leads to

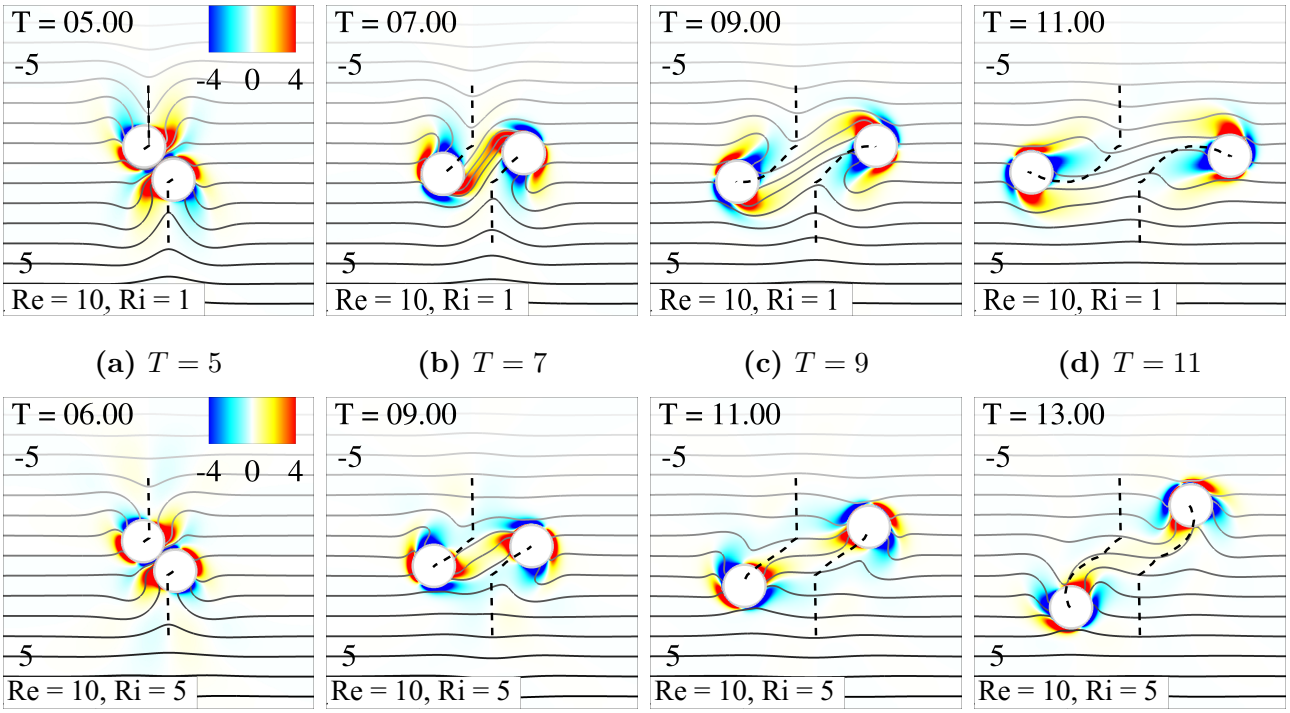

(a) $T = 5$ **(b)** $T = 7$ **(c)** $T = 9$ **(d)** $T = 11$

(e) $T = 6$ **(f)** $T = 9$ **(g)** $T = 11$ **(h)** $T = 13$

FIG. 3 Vorticity contours and isopycnals during the collision process of two approaching pullers with Re = 10 at different stratification strengths, Ri = 1 (a,b,c,d) and 5 (e,f,g,h). These plots show the interaction between the rear vorticity bubbles and the deformed isopycnals. The need of the displaced isopycnals to return to their original levels explain the rotational motion of the pullers after the collision. The isopycnals are the normalized density differences given by $(\rho - \rho_0)/\gamma a$ and each line is 1 unit apart. Darker shade of the line color indicates a higher density value. Colorbar for the vorticity contours is presented in the plots. The dashed lines show the trajectory of the pullers. These are snapshots of the flow-field at different dimensionless times, $T = tU_0/a$, the value of which is indicated in the caption. Colorbar is only shown in the first plot of each row for the neatness of the plots. For movies see [67].

reduction in the scattering angle of the squirmers after collision compared to their scattering angles in a homogeneous fluid as can be seen in fig. 2a, and 2b. For Re = 1 (Fig. 2a), stratification reduces ϕ from $\approx 45°$ in a homogeneous fluid to 0° for a stratified fluid with Ri = 10. For Re = 5, ϕ reduces to 0° for Ri = 10 from $\approx 90°$ for a homogeneous fluid. Thus, at low inertia, high enough stratification leads to the reorientation of the pullers to

their original orientation after the collision unlike in a homogeneous fluid.

For higher Re = 10, stratification leads to the elimination of the rotating motion of the pullers in clockwise loops present in a homogeneous fluid (see fig. 2c). For Re = 10, pullers are no more hydrodynamically trapped in the presence of density stratification unlike in the homogeneous fluid. They scatter away from each other with a positive scattering angle much like lower Re cases which decreases with an increase in the stratification strength. Again, high enough stratification strength leads to the reorientation of the pullers to their original orientation (see fig. 2c). For Re = 50, only a high stratification results in the elimination of the clockwise loops in the trajectories of the pullers after the collision. This is clear from the trajectories of pullers with Re = 50 in a stratified fluid with Ri = 10 (fig. 2d). The pullers escape from each other but with a large scattering angle which is greater than 90°. However, a lower stratification (Ri = 1 and 5) leads to the hydrodynamic trapping of the pullers after the collision in this case which is similar to the Re = 10 case in a homogeneous fluid.

To explain the reorientation of the pullers after the collision, the elimination of the closed loop trajectories and the prevention of the hydrodynamic trapping of the pullers we plot the vorticity contours and isopycnals at different time instances during the collision process of the pullers for two stratification strengths in fig. 3. The effect of increasing the inertia (or Re) of pullers is to increase the size of the vorticity bubble in the rear part of their bodies [26]. Introducing stratification reduces the size of these recirculatory regions behind pullers [38]. The trapping of the pullers in loops after the collision in a homogeneous fluid can be explained by the interaction between the bigger recirculatory regions behind the pullers at higher Re = 10 and 50 [27]. Since stratification leads to shrinking in the size of these rear recirculatory regions, the interaction between these rear bubbles is limited at finite Ri values. This prevents the pullers to attain a constant angular velocity after the collision unlike the homogeneous case (see fig. 4b). This damping of the angular velocity of the pullers after collision essentially allows the pullers to scatter away from each other without being trapped in counterclockwise loops. This point becomes clear from fig. 3 where we plot the vorticity contours and isopycnals for Re = 10 in stratified fluids with different stratification strengths, Ri = 1 and Ri = 5, respectively.

As the pullers move down (up) in a stratified fluid, they trap lighter (heavier) fluid in their rear recirculatory bubbles which can be seen in terms of deformed isopycnals in fig. 3.

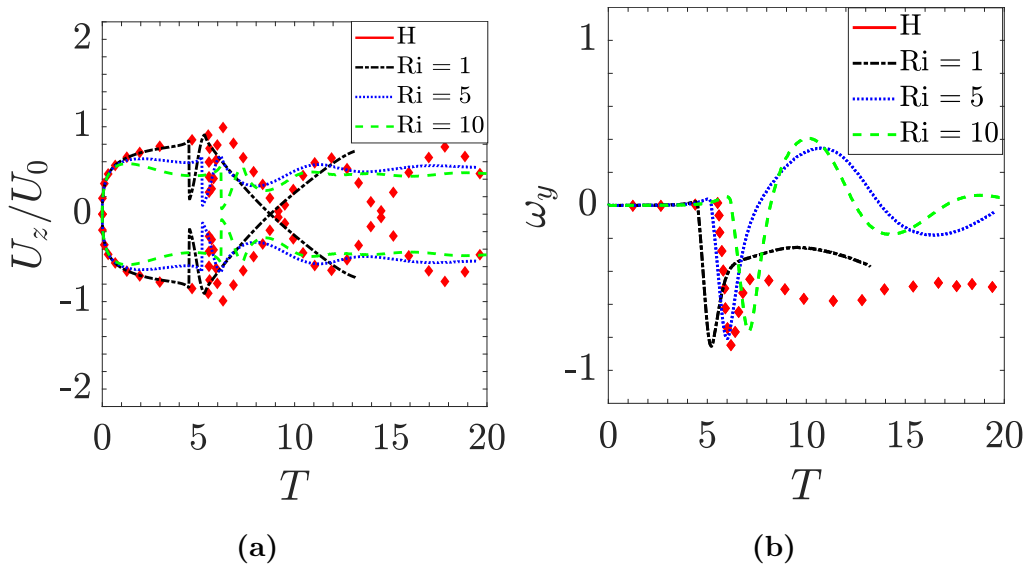

FIG. 4 Time evolution of the a) translational velocity and the b) rotational velocity of two approaching pullers during the collision process at different Ri values for a fixed Re = 10. Stratification eliminates the oscillations in the translational velocity and prevents the pullers from attaining a constant angular velocity thus eliminating the close loop trajectories as observed in the case of a homogeneous fluid. Stratification also results in a change in the sign of the angular velocity which reorients the pullers in their original orientations after the collision at high enough Ri.

After the collision, the axisymmetry of the flow and the isopycnal deformations is broken. The interaction between the rear vorticity bubbles rotates the pullers in clockwise direction as can be seen in fig. 3b. However, the tendency of the deformed isopycnals behind the pullers to return to their original positions reduces the effect of this interaction on the puller orientations (fig. 3f). The counterclockwise torque due to the flow induced by need of the deformed isopycnals to return to their original positions determines the rotational motion of the pullers after the collision and leads to the reorientation of the pullers in the original orientation. This prevents them from getting trapped into loops. This is clear from the comparison of the isopycnal deformation in fig. 3c and 3g.

At high Ri, i.e., Ri = 5 as compared to Ri = 1, the isopycnals are less deformed indicating that the resistance to the displacement of the isopycnals due to the flow induced by the squirmers is stronger. This prevents the clockwise rotation of the pullers and reorients them. Thus, the competition between the rear vorticity bubble interactions and the tendency of

deformed isopycnals to return to their original levels determines the rotational motions and the orientations of the pullers after the collision. Owing to the smaller size of the rear vorticity bubbles of pullers in a stratified fluid compared to a homogeneous fluid [38], the effect of the stratification dominates the vorticity bubble interactions between the two pullers at high Ri values. This prevents the pullers from attaining a constant angular velocity unlike in a homogeneous fluid, thus, eliminates the closed loops for Re = 10, 50 and results in the reorientation of the pullers for Re = 1, 5 and 10.

The consequences of the mentioned vorticity and isopycnal interactions on the colliding pullers can be understood from their translational and angular velocities. Velocity evolution for two approaching pullers is plotted in fig. 4 for Re = 10 and various stratification strengths. Stratification leads to the elimination of the oscillations in the translational velocities of the pullers after the collision and allows them to attain a steady velocity which results in their escape from each other (fig. 4a). In addition, the tendency of the displaced isopycnals to return to their neutrally buoyant levels prevent the pullers from attaining a constant angular velocity as can be seen in fig. 4b. This results in the reorientation of the pullers to their original orientation.

2. Pullers moving side by side

In addition to squirmers approaching each other in the opposite directions and colliding, we also investigate the motion of a pair of squirmers moving side by side initially apart by Δx in the x-direction. Fig. 5 shows the trajectories of two pullers moving side by side in different stratification strengths at Re = 10 and 50. In a homogeneous fluid, pullers moving side-by-side exhibit completely disparate trajectories at Re = 10 and Re = 50. At Re = 10, the pullers are initially attracted towards each other and they come close and stick together while they move downward. They move away from each other but are pulled together after a while. They again move down together a little before being repelled away from each other and finally scatter away in the horizontal direction (see fig. 5a). While for Re = 50, the pullers are slightly repelled from each other initially. But they are pulled towards each other which also leads to a torque on them making them rotate in a loop while they move down (see fig. 5b). Thus, in a homogeneous fluid, a pair of pullers moving side-by-side scatter away from each other at Re = 10 while they are hydrodynamically trapped near each other

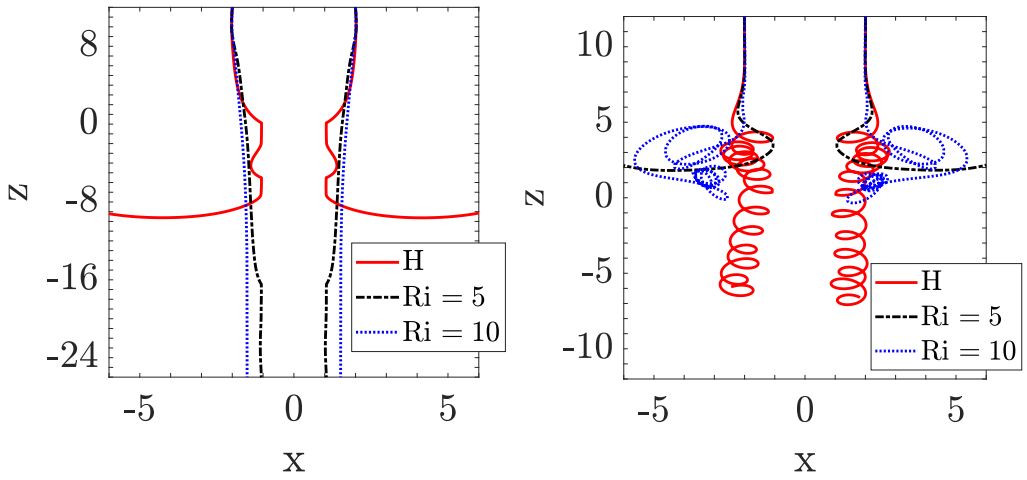

(a) Re = 10 **(b)** Re = 50

FIG. 5 Trajectories of a pair of pullers, $\beta = 5$, moving side-by-side initially separated by a distance $4a$ in x direction at various stratification strengths. a) Re = 10, b) Re = 50. H in the legends stands for homogeneous fluid or Ri = 0.

in loops for Re = 50.

Introducing stratification increases the attraction between the pullers moving side-by-side at Re = 10 (see fig. 5a). At Ri = 5 and 10, this increase in the attraction between the pullers increases the time that the pullers spend near each other before they collide and prevents the pullers from separating unlike in a homogeneous fluid. As a result, once the pullers collide sideways they stick together and move further down.

The significant changes in the trajectories of two pullers moving side-by-side due to stratification can also be seen at a higher Re (= 50, see fig. 5b). For Ri = 5, the pullers are again hydrodynamically trapped near each other in loops but they do not move much in the downward direction. Increasing the stratification further to Ri = 10, the pullers are attracted towards each other leading to a sideways collision. However, after this collision, they are repel away from each other and scatter away in the horizontal direction, similar to what happens eventually for Re = 10 in a homogeneous fluid. This is expected as stratification leads to a reduction in the squirmer velocities. This reduces their effective Re which explains the qualitative similarities between the trajectories in the high Re-high Ri and the low Re-no stratification case.

B. Pairwise interactions of pushers in a stratified fluid

1. *Pushers approaching each other*

Fig. 6 shows the trajectories for two pushers approaching each other in opposite directions, initially oriented parallel to each other for Re = 1, 5, 10 and 50 in a homogeneous fluid and a stratified fluid with different Ri. In the absence of any density stratification, the trajectories of the colliding pushers reveal two patterns based on the magnitude of Re. At relatively low values of Re, i.e., 1, the pushers come to a complete stop after the collision. However, this configuration is unstable and the pushers are deflected away from the $y = 0$ plane resulting in a three-dimensional (3D) motion after the collision [27]. This behavior is common for interacting pushers for Re $<<$ 1 and is due to the instability in their two-dimensional (2D) motion once they come close to each other [14]. As we increase the Re further, the pushers escape each other after the collision with a scattering angle $\phi < 90°$. ϕ increases with increase in the inertia of the pushers with values $\approx 0°$, $\approx 30°$ and $\approx 90°$ for Re = 5, 10 and 50, respectively.

Introducing stratification results in distinct changes in the trajectories of the interacting squirmers depending on their Re and the stratification strength, i.e., Ri. At low Re, the effect of introducing stratification on the trajectories of colliding pushers is to trap them near each other by bringing them to a complete stop. However, these states are not stable and soon the pushers leave the plane of collision, i.e., xz plane, and are deflected in the y direction. The pushers stick together as they leave the $y = 0$ plane and continue to move together in the y direction as shown in the insets of fig. 6a and 6b. The same is true for a high enough stratification at higher Re. The pushers come to a stand-still after collision and move together in the y plane for Re = 10 at Ri = 10. Introduction of the stratification leads to the reduction in the translational velocities of the pushers which reduces their effective inertia resulting in low Re like trajectories even at high Re values.

For intermediate Re = 10 and high Re = 50, the effect of stratification depends on the magnitude of Ri. The trapping due to the stoppage of the pushers after the collision at low Re values and the 3D trajectories are progressively prevented at high Re values. This can be seen in fig. 6c and 6d. At high Re and low Ri, the effect of inertia is significant compared to the effect of stratification. As a result, the pushers try to move away from each other

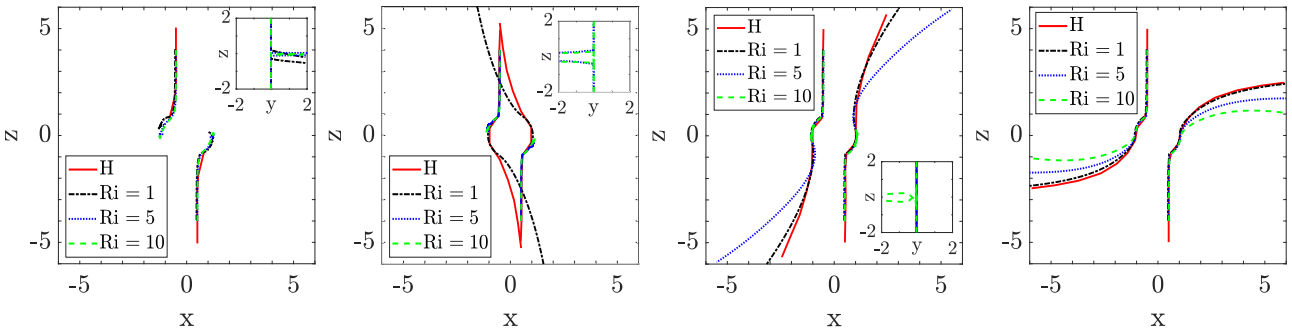

(a) Re = 1 **(b)** Re = 5 **(c)** Re = 10 **(d)** Re = 50

FIG. 6 Trajectories for colliding pushers with $\beta = -5$ in a homogeneous and a stratified fluid with increasing stratification strengths. At low Re = 1, 5 and 10, high enough stratification leads to the stoppage of the pushers as they collide. This state is not stable and as a results the pushers are deflected away from the xz plane in the y direction. The pushers stick together as they are move in the y direction after the deflection indicating that stratification leads to hydrodynamic trapping of colliding pushers. This deflection away from the xz plane is shown in the insets in (a), (b) and (c). This instability is gradually prevented with increasing Re and the pushers no more stop or are deflected at high Re, i.e., Re = 50. H in the legends stands for homogeneous fluid.

similar to what happens in a homogeneous fluid. This can be observed for Re = 10 at Ri = 1 & 5 and Re = 50 at Ri = 1, 5 & 10 for which pushers are scattered away from each other with $\phi \approx 45°$ and 90°, respectively.

We plot the vorticity contours and the isopycnals in fig. 7 for Re = 10 at two Ri values, viz., 1 and 5. The interaction of the pushers with the isopycnals reveal the reason behind the deflection from their trajectories in a homogeneous fluid for high Re values (10 and 50). Fig. 7 shows that as the pushers move forward, they displace the isopycnals behind them owing to the long vorticity trail behind them. However, as Ri increases these displaced isopycnals resist the flow induced by the pushers as they try to return to their original levels. The strength of opposition by the displaced isopycnals to their further deformation increases with Ri. E.g., for Ri = 1 (fig. 7a - 7d) the isopycnals behind the pushers are deformed for a longer time while they return to their original levels quickly for Ri = 5 (fig. 7e - 7h). As a result of the interaction between rear vorticity bubbles and the flow due to the deformed

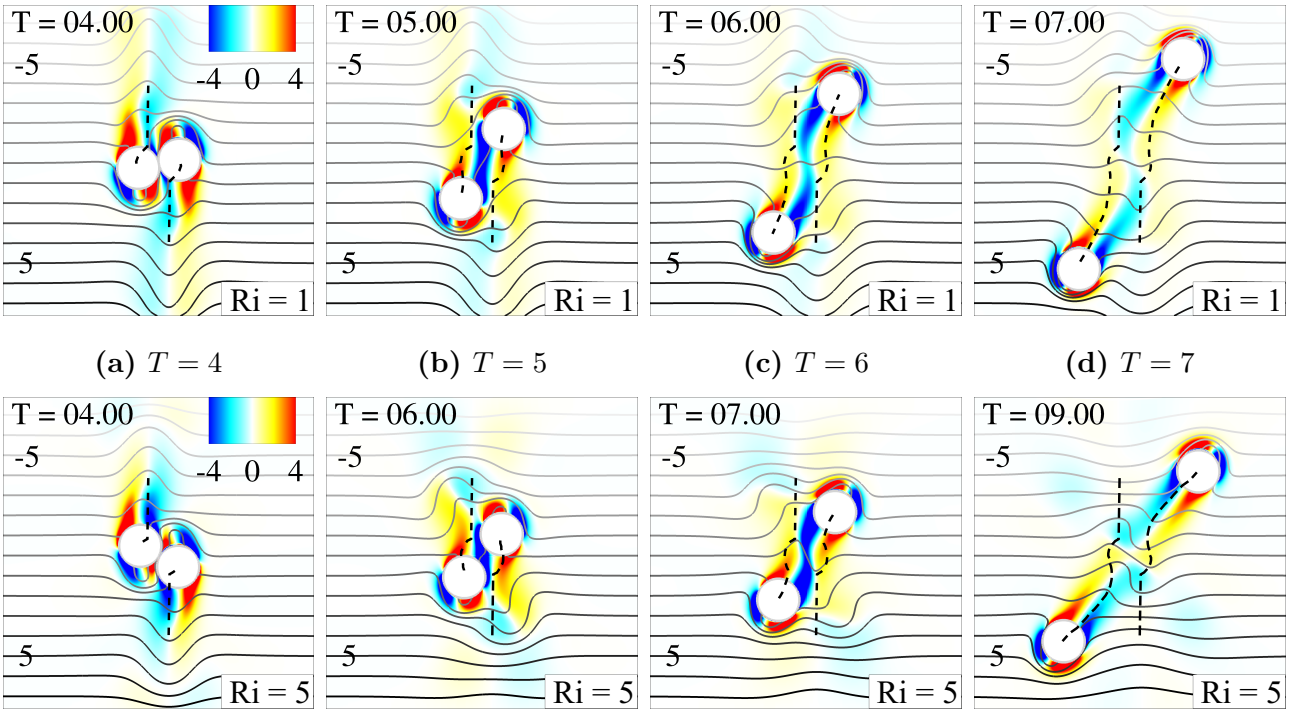

(a) $T = 4$ **(b)** $T = 5$ **(c)** $T = 6$ **(d)** $T = 7$

(e) $T = 4$ **(f)** $T = 6$ **(g)** $T = 7$ **(h)** $T = 9$

FIG. 7 Vorticity contours and isopycnals during the collision process of two approaching pushers with Re = 10 at different stratification strengths, Ri = 1 (a,b,c,d) and 5 (e,f,g,h). These plots show the interaction between the vorticity bubbles and the deformed isopycnals. The need of the displaced isopycnals to return to their original levels determine the trajectories of the pushers after the collision. The isopycnals are the normalized density differences given by $(\rho - \rho_0)/\gamma a$ and each line is 1 unit apart. Darker line color shade indicates a higher density value. Colorbar for the vorticity contours is presented in the plots. Dashed lines indicate the pusher trajectories. These are snapshots of the flow-field at different dimensionless times, $T = tU_0/a$, the value of which is indicated in the caption. Colorbar is only shown in the first plot of each row for the neatness of the plots. For movies see [67].

isopycnals in the wake of the pushers, their y angular velocity increases (see fig. 8b) and the pushers are deflected to their right.

Fig. 8 shows the translational and rotational velocities of the pushers at various stratification strengths for Re = 10. It can be seen from fig. 8a that the translational velocities of the squirmers decrease with increasing stratification both before and after the collision.

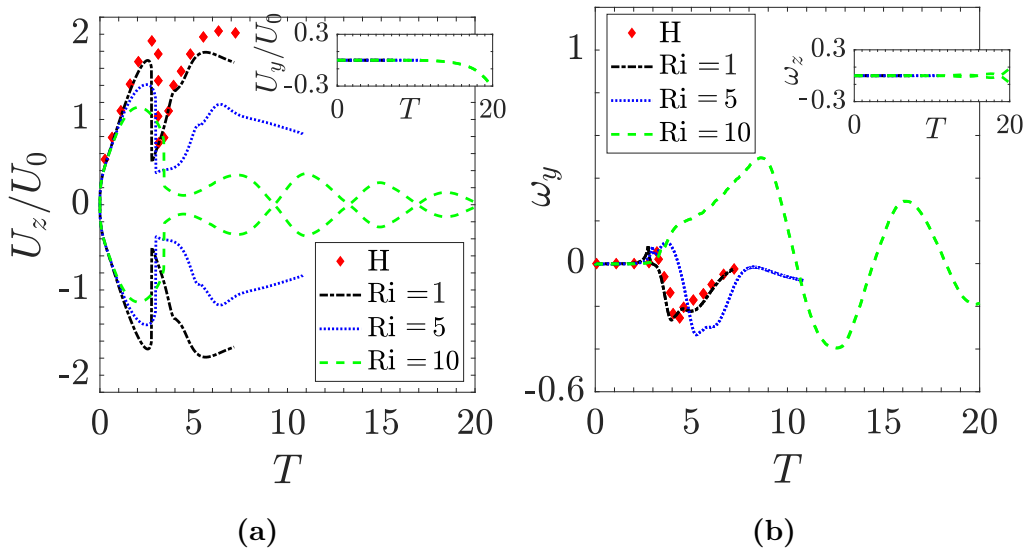

FIG. 8 Time evolution of the a) translational velocity and the b) rotational velocity of two approaching pushers during the collision process at different Ri values for a fixed Re = 10. Stratification leads to a significant reduction in the velocities of the pushers after their collision. At a high stratification, the pushers come to almost a stop after collision and eventually are deflected away from the $y = 0$ plane which is shown by the time evolution of the y velocities of the pullers in the insets.

The reason for this decrease is the trapping of lighter (heavier) fluid in the recirculatory region which in the front region leading to a higher buoyancy force on them as they move in a heavier (lighter) fluid. For a high enough Ri value (e.g. Ri = 10 at Re = 10) the velocity reduction is large enough to lead to an instability which deflects them away from the $y = 0$ plane. For the cases when the collision process does not lead to an instability (e.g., Ri = 1 and 5 at Re = 10), stratification increases the magnitude of the rotational velocity of the pushers which causes the divergence in their trajectories after the collision compared to their homogeneous fluid trajectories (see fig. 8b).

2. Pushers moving side by side

In contrast to a pair of pullers moving side-by-side, stratification has a limited effect on the trajectories of a pair of pushers moving side-by-side which is shown in fig. 9. For all the Re values explored, i.e., 10 and 50, the pushers are initially attracted towards each

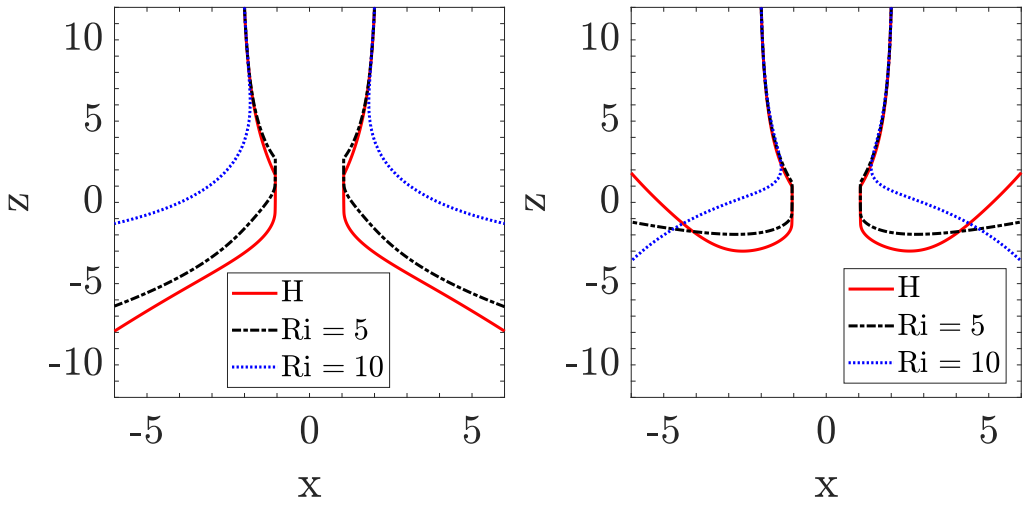

(a) Re = 10 **(b)** Re = 50

FIG. 9 Trajectories of a pair of pushers, $\beta = -5$, moving side-by-side initially separated by a distance $4a$ in x direction at various stratification strengths. a) Re = 10, b) Re = 50. H in the legends stands for homogeneous fluid or Ri = 0.

other. But this attraction does not last very long and eventually they deflect away from each other. The effect of stratification is to lower the z value where the pushers first start to separate from each other. Here we measure the scattering angle as the angle the final pusher orientation makes with its initial orientation.

In a homogeneous fluid, the pushers are attracted to each other at Re = 10 and 50. As they come very close, they stick together and move down before deflecting away. Increasing the inertia of the pushers leads to an increase in their scattering angle after the deflection (see fig. 9). Increasing the stratification strength hastens the process of repulsion leading to the pushers are pushed away at lower z distances from their initial positions as compared to a homogeneous fluid. At a high stratification, the pushers are pushed away from each other even before they can come very close to each other as they do in a homogeneous fluid. This is observed from the pusher trajectories at Ri = 10 for both Re values in fig. 9. In addition, at Re = 50, increasing the stratification leads to a reduction in the scattering angles of the pushers. However, at Re = 10, stratification results in a slight increase in the scattering angles of the pushers. Again, there are qualitative similarities in the trajectories of the pushers at high Re-high Ri and low Re-no stratification values as we observed in the case of a pair of pullers which is due to the reduction in the effective Re of the pushers at

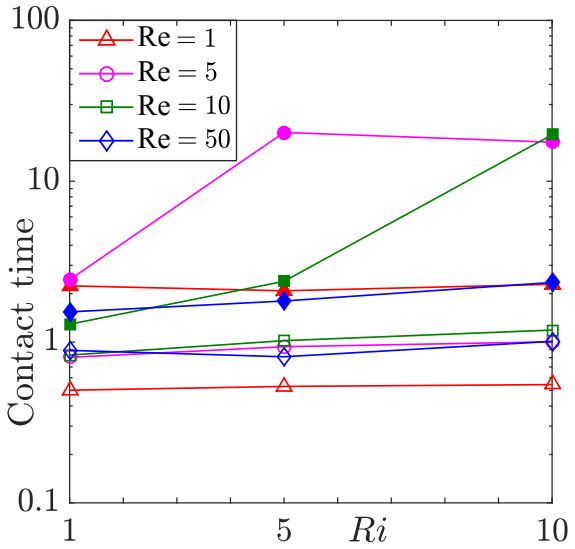

FIG. 10 Contact time, i.e., time spent by the squirmers near (center-to-center distance ≤ 2.12) each other for colliding squirmer pairs. Hollow symbols are for pullers and filled symbols are for pushers.

high Ri due to the reduction in their swimming speeds.

C. Contact time:

Fig. 10 plots the contact time for a pair of squirmers colliding with each other against Ri for various Re values explored in this study. We define contact time as the time spent by the squirmers in contact, i.e., when their center-to-center distance is less than $d + 2\Delta$ which is also the distance when the repulsive force between the squirmers is active. For the cases where the squirmers deflect away from the $y = 0$ plane, we measure contact time just before the squirmers are deflected. We observe that pushers spend more time in contact as compared to pullers for the range of parameters explored in this study. The contact time increases slightly with Ri for all the cases except for pushers with Re = 5 & 10. This is because the pushers are separated from each other at low Ri while they are trapped and deflect in the third direction at high Ri for Re = 5 & 10.

In many real-life situations, it is beneficial to estimate the contact time of swimmers. For reproductive purposes, it is beneficial for the swimmers to spend more time on contact while

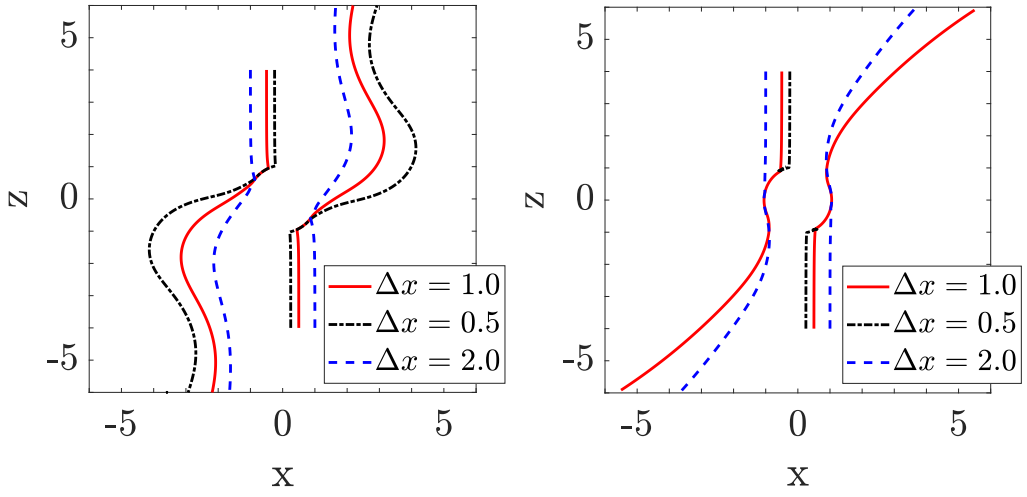

(a) Pullers, $\beta = 5$ **(b)** Pushers, $\beta = -5$

FIG. 11 Trajectories of a pair of colliding a) pullers, $\beta = 5$ and b) pushers, $\beta = -5$ For different Δx. Re = 10 and Ri = 5.

they want to not be in contact with a predator and escape as soon as possible. The results thus can be used to predict the encounter time of pusher and puller swimmers to predict their success in reproduction or feeding or escaping from predators. These results show that pushers tend to spend more time in contact than pullers which increases with increasing the stratification. This can enhance their success in reproduction in stratified environments.

D. Effect of initial lateral spacing:

Fig. 11 shows the effect of changing Δx on the trajectories of a pair of colliding squirmers for Re = 10 and Ri = 5. These results show that changing Δx for pullers does not change the trajectories of the pullers significantly as they are qualitatively the same. However, Δx has a significant role in determining the trajectories of colliding pushers. For $\Delta x = 1$ & 2 the pushers collide and separate from each other, while for a smaller Δx (=0.25), the pushers stop after the collision which is similar to what happens for high stratification at larger Δx. Thus, decreasing Δx simply decreases the Ri above which the instability in the colliding squirmer configuration sets in. Thus, the details of the trajectories are more closely related to the initial configuration for pushers than pullers.

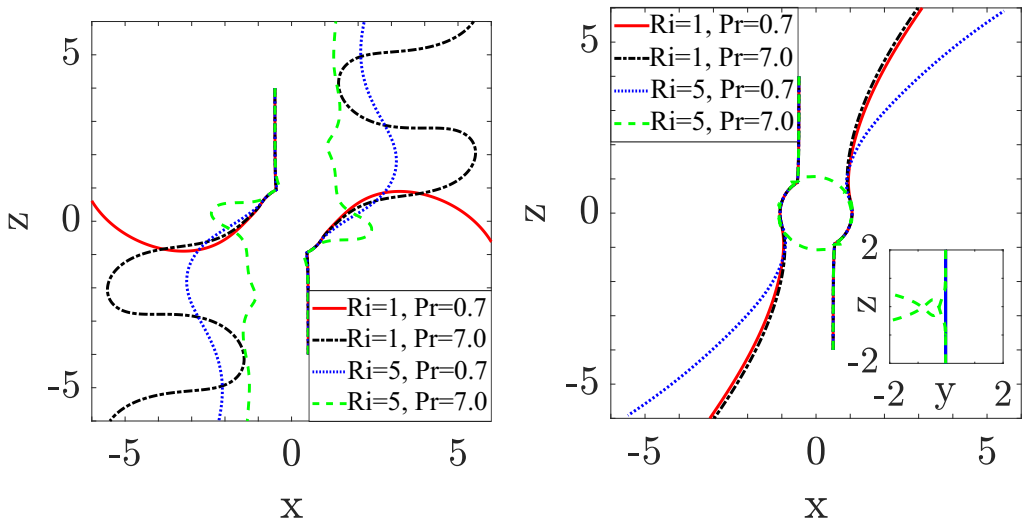

(a) Pullers, $\beta = 5$ **(b)** Pushers, $\beta = -5$

FIG. 12 Trajectories of a pair of pushers, $\beta = -5$, moving side-by-side initially separated by a distance $4a$ in x direction at various stratification strengths. a) Re = 10, b) Re = 50. H in the legends stands for homogeneous fluid or Ri = 0.

E. Effect of Prandtl number:

We briefly discuss the effects of varying Pr on the trajectories of colliding pair of pullers and pushers in this subsection. We assumed Pr = 0.7 for this study in order to resolve the density boundary layer. But for temperature stratified water Pr = 7 while Pr = 700 for salt stratified water. Resolving the density boundary layer ($\approx O(d/\sqrt{\mathrm{RePr}})$) becomes computationally expensive with increasing Pr. Hence a small value of Pr was used to save the computational penalty. Changing Pr of the fluid quantitatively changes the settling velocity of a rigid sphere [46] and the swimming velocity of neutrally buoyant squirmers [38] while the qualitative trend remains the same in both these cases. Thus, changing Pr will also change the trajectories of a pair of squirmers interacting in a stratified fluid. In addition, the transition from one type of trajectory to the other will happen at different values of Re and Ri.

We present the trajectories of a pair of pullers and pushers colliding for two different Ri and Pr in fig. 12. For a pair of colliding pullers with Re = 10, the pullers swim away from each other even at Pr = 7, however, their trajectories are different compared to Pr = 0.7 case. On the other hand, for pushers, the trajectories are similar for a lower Ri. But the

swimmers get trapped near each other for Ri = 5 in the case of Pr = 7 unlike the case when Pr = 0.7. These results show that the details of the trajectories, i.e., Ri for which they separate, exact trajectories and Ri for which they get trapped near each other and deflect away from the initial plane, depend on the value of Pr. This is expected as Pr governs the size of the density boundary layer which has an important role in determining the near field interactions between swimmers.

IV. CONCLUSIONS:

We investigate the interactions of a pair of squirmers with finite inertia in a stratified fluid with different stratification strength. We compare the squirmer trajectories and velocities with their trajectories and velocities in a homogeneous fluid for the same initial conditions. We present results for two types of initial configurations: 1) squirmers approaching each other in opposite directions, and 2) squirmers moving side-by-side in the vertical direction. The results presented can potentially be important in understanding the collective dynamics of microorganisms in oceans and lakes where stratification is observed.

For a pair of pullers approaching each other, stratification leads to their reorientation after the collision contrary to what happens in a homogeneous fluid. The tendency of the displaced isopycnals behind the pullers results in a torque on the pullers which reorients the pullers in their initial orientation after the collision. Stratification also leads to the elimination of the closed loop trajectories observed for colliding pullers at high Re (= 10 and 50) which has been explained using the flow field and the density field around the pullers during and after the collision.

A pair of pullers moving side-by-side follow complicated and distinct trajectories at different Re and Ri. In a homogeneous fluid, the pullers are repelled away from each other after initial attraction and a close contact for Re = 10, but they are hydrodynamically trapped near each other in loops as they move down for Re = 50. Again, high stratification leads to the elimination of the loops and hydrodynamic trapping deflecting the pullers away from each other even at Re = 50 similar to what happens for Re = 10 pullers in a homogeneous fluid.

A pair of pushers come to a complete stop after the collision at high Ri. However, this configuration is unstable which results in a 3D motion of the pushers away from the plane

of collision. As the pushers move away from the plane of collision, they stick together. The 3D motion is gradually prevented as we increase Re and a higher Ri is required for the instability. These results indicate that in a stratified fluid, organisms might get trapped near each other and move horizontally which can lead to their accumulation in oceans [41, 42].

In a homogeneous fluid, two pushers moving side-by-side are attracted towards each other, but eventually, they scatter away from each other with a scattering angle increasing with Re. Stratification hastens the repulsion between the pullers moving side-by-side and results in a decrease in the scattering angle at high Re.

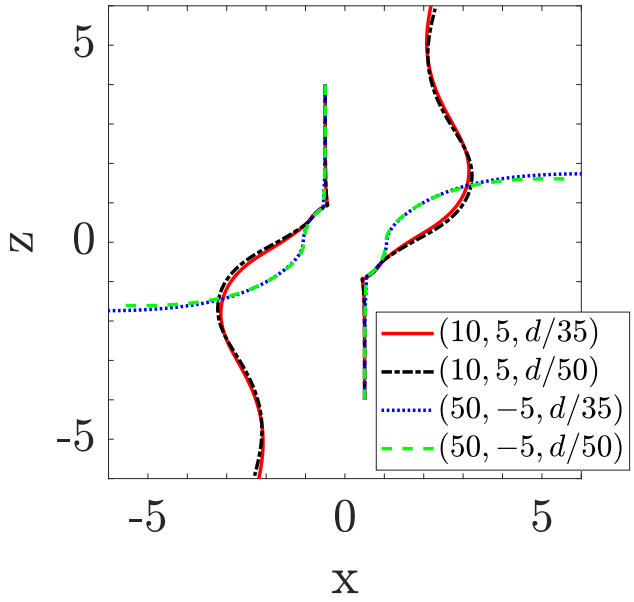

FIG. 13 Trajectories of a pair of colliding squirmers at two different grid resolutions. Legends are for (Re, β, Δ). Here Ri = 5 for all the cases.

The results for contact time for the squirmers show that pushers tend to spend more time in contact with each other than pullers. Furthermore, stratification increases the contact time for the squirmers. This indicates an enhanced chance for their success in reproduction in stratified environments. We also present results for variation in the Pr of the fluid and different lateral initial separations of the squirmers. But these were limited to a few cases to save computational expenses. Logical extensions of this work are to study the effects of varying the fluid Pr, the effects of squirmer swimming mode β, effects of initial squirmer configurations, and the effects of buoyancy by relaxing the quasi-instantaneous neutral buoyancy condition on the interactions of squirmers in a stratified fluid.

ACKNOWLEDGMENTS

The authors would like to acknowledge financial support from National Science Foundation via grants CBET-1604423, CBET-1700961, and CBET-1705371. This work used the Extreme Science and Engineering Discovery Environment (XSEDE) [68], which is supported by the National Science Foundation grant number ACI-1548562 through allocations TG-CTS180066 and TG-CTS190041.

Appendix A: Grid and domain independence

We present the grid independence test results in this appendix. Fig. 13 shows the trajectories for a pair of squirmers approaching each other in opposite directions for two different grid sizes. As can be seen in the figure, changing the grid size from $\Delta = d/35$ to $\Delta = d/50$ results in a negligible variation in the trajectories of the colliding squirmers. Here, Δ is the smallest grid size. Hence, to save the computational cost, we carried all the simulations with $\Delta = d/35$. Further validations for the homogeneous fluid cases can be found in Ref. [27].

[1] C. Dombrowski, L. Cisneros, S. Chatkaew, R. E. Goldstein, and J. O. Kessler, Self-concentration and large-scale coherence in bacterial dynamics, Physical review letters **93**, 098103 (2004).

[2] H. H. Wensink, J. Dunkel, S. Heidenreich, K. Drescher, R. E. Goldstein, H. Löwen, and J. M. Yeomans, Meso-scale turbulence in living fluids, Proceedings of the National Academy of Sciences **109**, 14308 (2012).

[3] A. Sokolov, I. S. Aranson, J. O. Kessler, and R. E. Goldstein, Concentration dependence of the collective dynamics of swimming bacteria, Physical review letters **98**, 158102 (2007).

[4] X.-L. Wu and A. Libchaber, Particle diffusion in a quasi-two-dimensional bacterial bath, Phys. Rev. Lett. **84**, 3017 (2000).

[5] F. E. Fish, Kinematics of ducklings swimming in formation: consequences of position, Journal of Experimental Zoology **273**, 1 (1995).

[6] B. S. Beckett, *Biology: a modern introduction* (Oxford University Press, USA, 1986).

[7] D. Saintillan and M. J. Shelley, Orientational order and instabilities in suspensions of self-locomoting rods, Physical review letters **99**, 058102 (2007).

[8] E. Lushi, H. Wioland, and R. E. Goldstein, Fluid flows created by swimming bacteria drive self-organization in confined suspensions, Proceedings of the National Academy of Sciences **111**, 9733 (2014).

[9] A. T. Chwang and T. Y.-T. Wu, Hydromechanics of low-reynolds-number flow. part 2. singularity method for stokes flows, Journal of Fluid mechanics **67**, 787 (1975).

[10] K. Drescher, K. C. Leptos, I. Tuval, T. Ishikawa, T. J. Pedley, and R. E. Goldstein, Dancing volvox: hydrodynamic bound states of swimming algae, Physical Review Letters **102**, 168101 (2009).

[11] T. Ishikawa and M. Hota, Interaction of two swimming paramecia, Journal of Experimental Biology **209**, 4452 (2006).

[12] X. Chen, X. Yang, M. Yang, and H. Zhang, Dynamic clustering in suspension of motile bacteria, EPL (Europhysics Letters) **111**, 54002 (2015).

[13] A. P. Petroff, X.-L. Wu, and A. Libchaber, Fast-moving bacteria self-organize into active two-dimensional crystals of rotating cells, Physical review letters **114**, 158102 (2015).

[14] T. Ishikawa, M. Simmonds, and T. J. Pedley, Hydrodynamic interaction of two swimming model micro-organisms, Journal of Fluid Mechanics **568**, 119 (2006).

[15] I. O. Götze and G. Gompper, Mesoscale simulations of hydrodynamic squirmer interactions, Physical Review E **82**, 041921 (2010).

[16] T. Ishikawa, G. Sekiya, Y. Imai, and T. Yamaguchi, Hydrodynamic interactions between two swimming bacteria, Biophysical journal **93**, 2217 (2007).

[17] G. Alexander, C. Pooley, and J. Yeomans, Scattering of low-reynolds-number swimmers, Physical Review E **78**, 045302 (2008).

[18] A. Furukawa, D. Marenduzzo, and M. E. Cates, Activity-induced clustering in model dumbbell swimmers: the role of hydrodynamic interactions, Physical Review E **90**, 022303 (2014).

[19] R. Maniyeri and S. Kang, Hydrodynamic interaction between two swimming bacterial flagella in a viscous fluid–a numerical study using an immersed boundary method, Progress in Computational Fluid Dynamics, an International Journal **14**, 375 (2014).

[20] C. Pooley, G. Alexander, and J. Yeomans, Hydrodynamic interaction between two swimmers at low reynolds number, Physical review letters **99**, 228103 (2007).

[21] G. J. Elfring and E. Lauga, Hydrodynamic phase locking of swimming microorganisms, Physical review letters **103**, 088101 (2009).

[22] C. Brennen and H. Winet, Fluid mechanics of propulsion by cilia and flagella, Annual Review of Fluid Mechanics **9**, 339 (1977).

[23] L. N. Wickramarathna, C. Noss, and A. Lorke, Hydrodynamic trails produced by daphnia: size and energetics, PloS one **9** (2014).

[24] T. Kiørboe, H. Jiang, and S. P. Colin, Danger of zooplankton feeding: the fluid signal generated by ambush-feeding copepods, Proceedings of the Royal Society B: Biological Sciences **277**, 3229 (2010).

[25] S. Wang and A. Ardekani, Inertial squirmer, Physics of Fluids **24**, 101902 (2012).

[26] N. G. Chisholm, D. Legendre, E. Lauga, and A. S. Khair, A squirmer across reynolds numbers, Journal of Fluid Mechanics **796**, 233 (2016).

[27] G. Li, A. Ostace, and A. M. Ardekani, Hydrodynamic interaction of swimming organisms in an inertial regime, Physical Review E **94**, 1 (2016).

[28] R. Ouillon, I. A. Houghton, J. O. Dabiri, and E. Meighburg, Active swimmers interacting with stratified fluids during collective vertical migration, Journal of Fluid Mechanics **902**, A23 (2020).

[29] S. MacIntyre, A. L. Alldredge, and C. C. Gotschalk, Accumulation of marines now at density discontinuities in the water column, Limnology and Oceanography **40**, 449 (1995).

[30] H. Yamazaki and K. D. Squires, Comparison of oceanic turbulence and copepod swimming, Marine Ecology Progress Series **144**, 299 (1996).

[31] A. L. Alldredge, T. J. Cowles, S. MacIntyre, J. E. Rines, P. L. Donaghay, C. F. Greenlaw, D. Holliday, M. M. Dekshenieks, J. M. Sullivan, and J. R. V. Zaneveld, Occurrence and mechanisms of formation of a dramatic thin layer of marine snow in a shallow pacific fjord, Marine Ecology Progress Series **233**, 1 (2002).

[32] S. Wang and A. M. Ardekani, Biogenic mixing induced by intermediate Reynolds number swimming in stratified fluids, Scientific Reports **5**, 10.1038/srep17448 (2015).

[33] R. More and S. Balasubramanian, Mixing dynamics in double-diffusive convective stratified fluid layers, Current Science **114**, 1953–1960 (2018).

[34] A. Ardekani and R. Stocker, Stratlets: Low reynolds number point-force solutions in a stratified fluid, Physical review letters **105**, 084502 (2010).

[35] J. S. Guasto, R. Rusconi, and R. Stocker, Fluid mechanics of planktonic microorganisms, Annual Review of Fluid Mechanics **44**, 373 (2012).

[36] A. Doostmohammadi, R. Stocker, and A. M. Ardekani, Low-reynolds-number swimming at pycnoclines, Proceedings of the National Academy of Sciences **109**, 3856 (2012).

[37] R. Dandekar, V. A. Shaik, and A. M. Ardekani, Swimming sheet in a density-stratified fluid, Journal of Fluid Mechanics **874**, 210 (2019).

[38] R. V. More and A. M. Ardekani, Motion of an inertial squirmer in a density stratified fluid, Journal of Fluid Mechanics **905**, A9 (2020).

[39] C. Noss and A. Lorke, Direct observation of biomixing by vertically migrating zooplankton, Limnology and oceanography **59**, 724 (2014).

[40] I. A. Houghton, J. R. Koseff, S. G. Monismith, and J. O. Dabiri, Vertically migrating swimmers generate aggregation-scale eddies in a stratified column, Nature **556**, 497 (2018).

[41] D. Viličić, T. Legović, and V. Žutić, Vertical distribution of phytoplankton in a stratified estuary, Aquatic Sciences **51**, 31 (1989).

[42] P. Hershberger, J. Rensel, A. Matter, and F. Taub, Vertical distribution of the chloromonad flagellate heterosigma carterae in columns: implications for bloom development, Canadian journal of fisheries and aquatic sciences **54**, 2228 (1997).

[43] R. Glowinski, T.-W. Pan, T. I. Hesla, D. D. Joseph, and J. Periaux, A fictitious domain approach to the direct numerical simulation of incompressible viscous flow past moving rigid bodies: application to particulate flow, Journal of Computational Physics **169**, 363 (2001).

[44] A. M. Ardekani, S. Dabiri, and R. H. Rangel, Collision of multi-particle and general shape objects in a viscous fluid, Journal of Computational Physics **227**, 10094 (2008).

[45] A. M. Ardekani and R. H. Rangel, Numerical investigation of particle–particle and particle–wall collisions in a viscous fluid, Journal of Fluid Mechanics **596**, 437 (2008).

[46] A. Doostmohammadi, S. Dabiri, and A. M. Ardekani, A numerical study of the dynamics of a particle settling at moderate Reynolds numbers in a linearly stratified fluid, Journal of Fluid Mechanics **750**, 5 (2014).

[47] W. Aniszewski, T. Arrufat, M. Crialesi-Esposito, S. Dabiri, D. Fuster, Y. Ling, J. Lu, L. Malan, S. Pal, R. Scardovelli, and G. Tryggvason, Parallel, robust, interface simulator (paris), (2019).

[48] B. P. Leonard, A stable and accurate convective modelling procedure based on quadratic upstream interpolation, Computer methods in applied mechanics and engineering **19**, 59 (1979).

[49] M. Lighthill, On the squirming motion of nearly spherical deformable bodies through liquids at very small reynolds numbers, Communications on Pure and Applied Mathematics **5**, 109 (1952).

[50] J. R. Blake, A spherical envelope approach to ciliary propulsion, Journal of Fluid Mechanics **46**, 199 (1971).

[51] T. Pedley, Spherical squirmers: models for swimming micro-organisms, IMA Journal of Applied Mathematics **81**, 488 (2016).

[52] V. Magar, T. Goto, and T. Pedley, Nutrient uptake by a self-propelled steady squirmer, The Quarterly Journal of Mechanics and Applied Mathematics **56**, 65 (2003).

[53] T. Ishikawa and T. Pedley, The rheology of a semi-dilute suspension of swimming model micro-organisms, Journal of Fluid Mechanics **588**, 399 (2007).

[54] J.-L. Thiffeault and S. Childress, Stirring by swimming bodies, Physics Letters A **374**, 3487 (2010).

[55] L. Zhu, E. Lauga, and L. Brandt, Self-propulsion in viscoelastic fluids: Pushers vs. pullers, Physics of fluids **24**, 051902 (2012).

[56] G.-J. Li, A. Karimi, and A. M. Ardekani, Effect of solid boundaries on swimming dynamics of microorganisms in a viscoelastic fluid, Rheologica acta **53**, 911 (2014).

[57] G.-J. Li and A. M. Ardekani, Hydrodynamic interaction of microswimmers near a wall, Physical Review E **90**, 013010 (2014).

[58] S. Wang and A. Ardekani, Unsteady swimming of small organisms, Journal of Fluid Mechanics **702**, 286 (2012).

[59] A. E. Walsby, Gas vesicles., Microbiology and Molecular Biology Reviews **58**, 94 (1994).

[60] T. A. Villareal and E. Carpenter, Buoyancy regulation and the potential for vertical migration in the oceanic cyanobacterium trichodesmium, Microbial ecology **45**, 1 (2003).

[61] C. Boyd and D. Gradmann, Impact of osmolytes on buoyancy of marine phytoplankton, Marine Biology **141**, 605 (2002).

[62] F. J. Sartoris, D. N. Thomas, A. Cornils, and S. B. S. Schiela, Buoyancy and diapause in antarctic copepods: the role of ammonium accumulation, Limnology and oceanography **55**, 1860 (2010).

[63] N. Sanders and J. Childress, Ion replacement as a buoyancy mechanism in a pelagic deep-sea crustacean, Journal of Experimental Biology **138**, 333 (1988).

[64] J. Luo, P. B. Ortner, D. Forcucci, and S. R. Cummings, Diel vertical migration of zooplankton and mesopelagic fish in the Arabian Sea, Deep Sea Research Part II: Topical Studies in Oceanography **47**, 1451–1473 (2000).

[65] D. K. Steinberg, B. A. Van Mooy, K. O. Buesseler, P. W. Boyd, T. Kobari, and D. M. Karl, Bacterial vs. zooplankton control of sinking particle flux in the ocean's twilight zone, Limnology and Oceanography **53**, 1327–1338 (2008).

[66] N. Hill and T. Pedley, Bioconvection, Fluid Dynamics Research **37**, 1 (2005).

[67] See supplemental material at, for the videos of a colliding pair of pushers and pullers in a stratified fluid.

[68] J. Towns, T. Cockerill, M. Dahan, I. Foster, K. Gaither, A. Grimshaw, V. Hazlewood, S. Lathrop, D. Lifka, G. D. Peterson, *et al.*, Xsede: accelerating scientific discovery, Computing in science & engineering **16**, 62 (2014).